Fabrication and Test of 90-mm Nb_3Sn Quadrupole Model Based on Dipole-type Collar

R. Bossert, N. Andreev, G. Chlachidze, V.S. Kashikhin, V.V. Kashikhin, M.J. Lamm, F. Nobrega, I. Novitski, M. Tartaglia, G. Velev, A.V. Zlobin

***Abstract*— A series of 90-mm TQC quadrupole models with a collar-based mechanical structure has been fabricated and tested within the framework of the US-LHC Accelerator Research Program (LARP) using quadrupole-symmetric stainless steel collar laminations. This paper describes the design features, construction and test of TQC02Eb, the first TQC made with dipole-type collar and collaring techniques. Magnet test includes quench performance and field quality measurements at 4.5 and 1.9 K. Results of model performance for TQC quadrupoles based on dipole-type and quadrupole-type collars are compared and discussed.**

***Index Terms*— Nb_3Sn quadrupole, dipole-type collar, magnet test.**

I. INTRODUCTION

FERMILAB is developing large-aperture high-gradient quadrupoles based on Nb_3Sn superconductor for a planned upgrade to the interaction regions (IR) of the Large Hadron Collider (LHC) [1] and other applications including Muon Collider IRs [2]. Several technological quadrupole (TQ) models [3-6] have been fabricated and tested at Fermilab within the framework of US LHC Accelerator Research Program (LARP) [7]. These models employ a conventional mechanical structure based on stainless steel collars similar to that used in NbTi accelerator magnets, including the LHC IR quadrupoles.

The collar has been a reliable system, providing the required coil geometry and alignment as well as pre-stress and support. Although the design is well-established for NbTi magnets, the TQ models represent the first attempt to use this method for Nb_3Sn coils. Quadrupole models of the TQC series based on traditional quadrupole collars have been fabricated and tested successfully, but due to the brittle conductor, the time required for the collaring process must be extended. To reduce construction time as well as minimize potential risks of damage to the coils, an alternative collaring technique using dipole-style collars has been implemented.

This paper describes the construction and testing of TQC02Eb, the first 1 meter model using the dipole system. These results are compared with TQC02Ea, an earlier model which utilized most of the same coils but was built with quadrupole-style collars, and several TQS02 models, also built with the same coils but a different (shell type) structure [8].

Manuscript received Aug 2, 2010.

Work supported by Fermi Research Alliance, LLC, under contract No. DE-AC02-07CH11359 with the U.S. Department of Energy.

Authors are with the Fermi National Accelerator Laboratory, Batavia, IL 60510 USA (corresponding author phone: 630-840-2867; fax: 630-840-3369; e-mail: bossert@fnal.gov).

II. TQC MODEL DESIGN AND FABRICATION

A. Quadrupole Collaring Concepts

The traditional quadrupole collaring system uses quadrupole-symmetric laminated collars. The collared coil assembly is positioned vertically in a four-jaw press, then compressed incrementally in the longitudinal direction, in sections 10-15 cm long, while a separate set of cylinders drives in keys to lock the collars together. This technique was successfully used at Fermilab to collar NbTi quadrupoles for the Tevatron and the LHC IRs, as well as Nb_3Sn models for LARP. When using this method for brittle Nb_3Sn, multiple passes are required to avoid large stress/strain variations at the boundary between compressed and non-compressed sections. In order to limit the maximum difference in azimuthal stress between adjacent sections to ~10-15 MPa, 6-8 passes are usually required to achieve the final target coil prestress. The duration of the collaring procedure for this approach is proportional to the coil length and usually takes about 1 week for 1 m long coils. The maximum magnet length for this technique is also limited by the vertical space in the magnet production facility (currently 6 meters).

An alternative method of collaring is based on a dipole-symmetric collar and utilizes a horizontal press, similar to the way superconducting dipoles are traditionally collared. This approach has also been successfully used for NbTi quadrupoles [9-11]. With this system, quadrupole coils are compressed simultaneously along their entire length, eliminating local stress gradients. This lowers the risk of Nb_3Sn coil damage resulting from incremental coil compression. It also significantly reduces the collaring process time as well as making it independent of length. Pictures of quadrupole and dipole style collar packs are shown in Fig 1. A detailed discussion of the design features and fabrication methods of both collaring systems has been previously presented [12].

B. TQC02E(a and b) Construction

Quadrupole models TQC02Ea and TQC02Eb were built with coils used previously in several TQS02 models. The baseline TQ coil design and technology are described in [3]. The cable was made using 0.7-mm Nb_3Sn RRP-54/61 strand based on the Rod Restack Process (RRP) by OST, and insulated with a 125 μm thick S2-glass sleeve. The coils have

Fig. 1. TQ collar blocks made of the quadrupole style (left) dipole-style (right) round collar.

titanium alloy poles. Coil combinations in TQC02 and TQS02 models, model assembly and test sequence, and average coil warm and cold pre-stresses are shown in Table 1.

Table 1. TQ assemblies with azimuthal prestress at different stages of assembly and testing

Model	Coils	Coil prestress average, MPa		
		collared	Final warm	cold
TQS02a	20,21,22,23	N/A	-40*	-155*
TQC02Ea	20,21,22,23	-51	-112	-112*
TQS02b	22,23,28,29	N/A	-40*	-155*
TQS02c	20,22,23,28	N/A	-40*	-155*
TQC02Eb	20,22,23,28	+8v/-31h	-124	-124*

*calculated using ANSYS.

TQC models are assembled in two stages. The first stage includes coil collaring using collar blocks. The second stage includes collared coil yoking and skinning. The collared coil provides an intermediate preload (approximately 30-50 MPa), while additional support from the yoke and skin through radial shims increases preload in the final assembly to 110-150 MPa. Over-compression during cooldown is prevented by the control spacer when using quadrupole style collars and by the collar surface for dipole style collars. The same yoke and bolted skin are used regardless of collar style. TQC cold mass assemblies of both types are shown in Figs. 2 and 3.

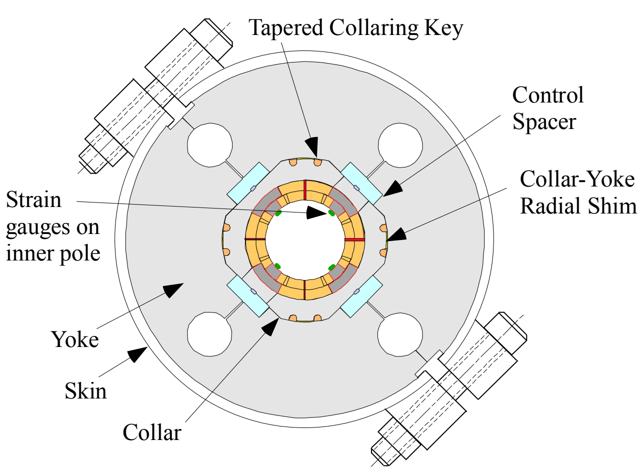

Fig. 2. TQC assembly with quadrupole-style collars as in TQC02Ea.

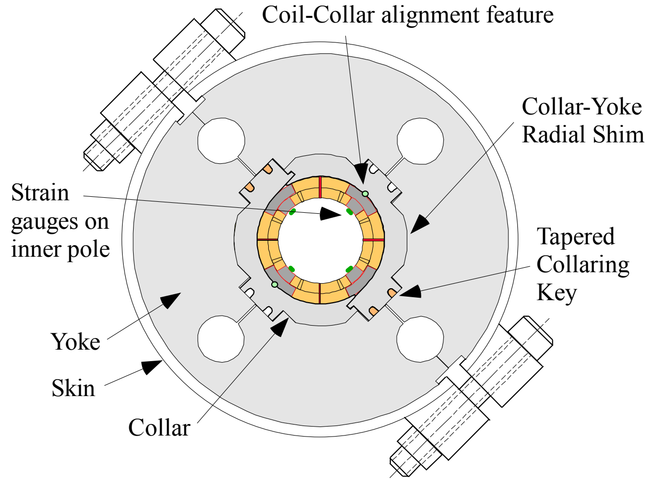

Fig. 3. TQC assembly with dipole-style collars as in TQC02Eb.

TQC02Eb also included a coil-to-collar alignment key shown in Fig. 3. This was incorporated into a TQC or TQS assembly for the first time. This feature can be used with either collar style.

Coil pre-stress as read by strain gauges placed on the inner metal pole surface after collaring and yoking is shown for TQC02Ea and TQC02Eb in Figure 4. During collaring using quadrupole-style collars, preload increased uniformly from coil-to-coil, while with the dipole-style collars, compressive stresses were much larger in the coils on the vertical axis than on the horizontal (in fact, positive “tensile” numbers are recorded on the horizontal axis). This is because the structure assumes a slightly vertically oval shape during the collaring process, and the strain gauges on the inner surface reflect bending from the oval condition. Collar deflections in the completed collared coil structure (Fig.5) confirm this ovality. The asymmetry was then completely eliminated during the yoking process, where the yoke support controls the shape of the collars.

The vertical ovality seen in TQC02Eb was due to two factors; errors in tolerances of the collar lamination key slots, and weakness of the collar structure [12]. It can be reduced significantly or completely eliminated by modification of the laminations and strengthening the packs by welding. Nevertheless, test results showed that the temporary small ovality during the assembly process does not damage the conductor.

Although the oval condition during collaring does not occur when using the quadrupole system, a more severe condition does take place. Large differences in prestress occur axially due to the incremental collaring. Since the cable is bent in the wide direction (“the hard way”), when collaring in the quadrupole manner, that process is potentially more damaging to the conductor.

The final completed assembly shows similar preloads whether dipole or quadrupole style collars are used (Fig 4).

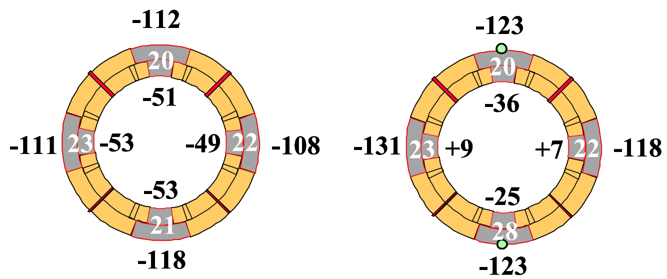

Fig. 4. TQC02Ea (left) and TQC02Eb (right) stresses at the four poles during assembly (in MPa), shown in orientation during construction. Preload after collaring is shown on inside of bore, and preload after yoking is shown on outside of bore. Coil production number is in white.

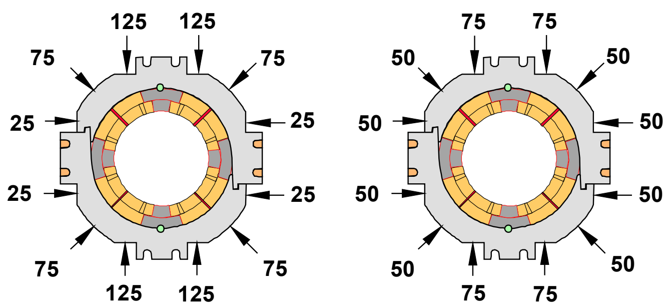

Fig. 5. Collar deflection measurements of TQC02Eb as measured (left) and after lamination stamping errors have been subtracted out (right). Numbers represent radial deflections in microns.

III. Test Results

TQC02Eb was tested in liquid He in Fermilab's Vertical Magnet Test Facility (VMTF). The magnet test plan included quench training and ramp rate studies both at 4.5 K and 1.9 K, temperature dependence studies and magnetic measurements. The reference TQC02Ea model with quadrupole style collars was tested in October of 2007. Magnet fabrication and test results are reported in [5].

TQC02Eb training quenches are shown in Fig. 6. After 12 quenches at 4.5K, the magnet quench current reached 12.6 kA or 210 T/m field gradient. At 1.9 K quench performance was erratic due to flux jump instabilities in Nb_3Sn strands, as was previously observed in TQC02Ea and other magnets made of RRP-54/61 strands. During temperature dependence studies the magnet showed training at 3.2 K as well and reached the maximum field gradient of 217 T/m. Training quenches mostly originated from the pole-turn blocks, but at the plateau quench location moved to the mid-plane blocks of the magnet.

TQC02Eb reached the highest critical current and field gradient among all magnets of the TQC series.

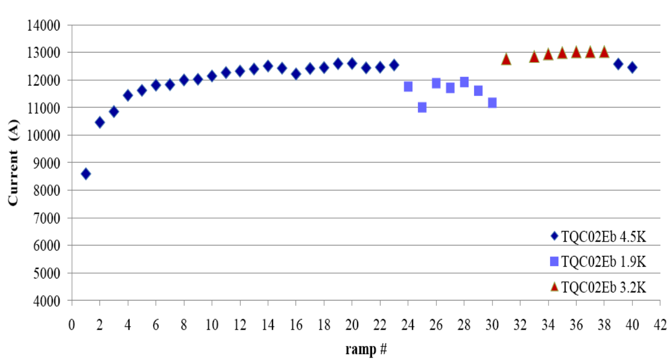

Fig. 6. TQC02Eb quench training

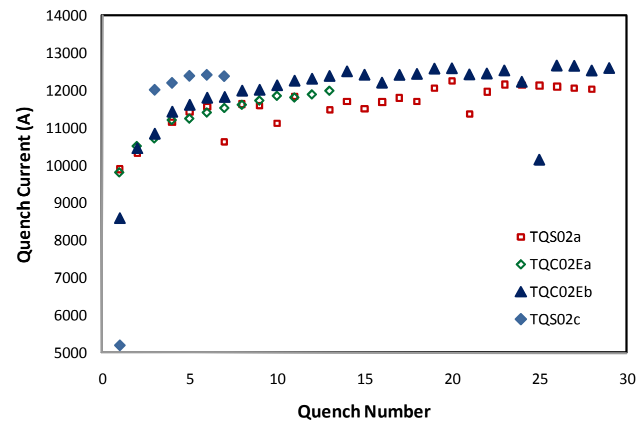

Fig. 7. Comparison of quench training at 4.5 K in TQC02Ea, TQC02Eb, TQS01a and TQS02c magnets

TQC02Eb quench performance at 4.5 K is compared with the performance of the TQC02Ea and TQS02a/c magnets in Fig. 7. One can see that the TQC02Eb quench performance is consistent with performance of both magnets. The dipole style collar design and assembly procedure used in TQC02Eb did not introduce any additional degradation or magnet training behavior. Moreover, this test after multiple handling and test cycles once again confirmed the robustness of Nb_3Sn coils.

Magnet ramp rate dependences at 4.5 K and 1.9 K are shown in Fig. 8. All quenches during ramp rate study originated from the mid-plane blocks. Whereas the high ramp rate quenches in the midplane turns are caused by eddy currents in the cable, the low ramp rate quenches in low field regions are likely due to the flux jump instabilities. At 1.9 K the flux jump quenches are seen at dI/dt<250 A/s. At 4.5 K they occur at dI/dt<100 A/s while the quench current is only a few percent lower that the coil short sample limit. At ramp rates below 150 A/s, the quench current at 1.9 K is lower than at 4.5 K. One can see similar features in the ramp rate dependences of TQC02Ea in Figure 8.

The temperature dependences of the TQC02Eb quench current for two different ramp rates (50 A/s and 200 A/s) are shown in Fig. 9. At 50 A/s, the quench current is clearly affected by the flux jump instabilities at T<4 K. At 200 A/s the flux jump instabilities are suppressed by AC losses in practically the entire temperature range from 1.9 to 4.5 K.

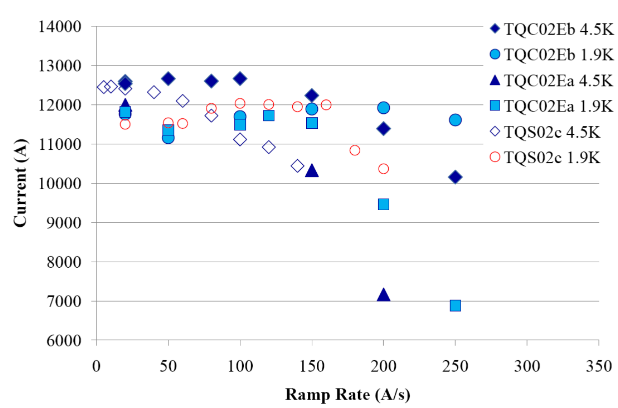

Fig. 8. TQC02Eb ramp rate dependence at 4.5 K and 1.9 K

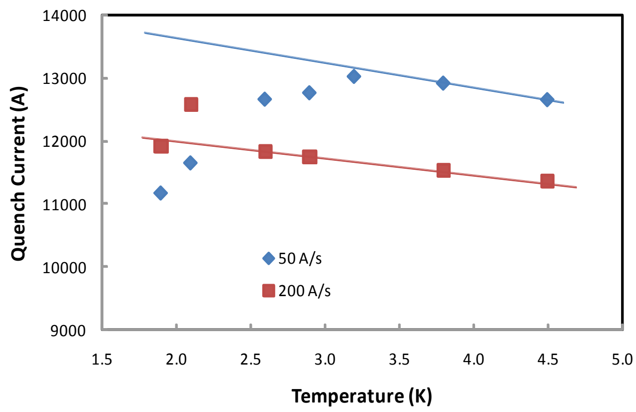

Fig. 9. TQC02Eb current vs. helium bath temperatures at two different current ramp rates.

TABLE 2 TQC02Eb (TQC02Ea) Body Harmonics (in units) at 100 T/m Field Gradient

n	b	a
3	-3.57 (-2.56)	4.71 (1.72)
4	-3.34 (-1.65)	-0.29 (-2.7)
5	0.20 (0.72)	-0.76 (1.61)
6	-0.62 (-0.96)	0.05 (0.59)
7	0.03 (-0.34)	0.10 (-0.32)
8	-0.07 (0.14)	0.01 (-0.07)
9	0.06 (0.06)	-0.02 (0.12)
10	0.01 (-0.08)	0.02 (-0.01)

Field quality magnetic measurements were made with the DSP rotating harmonic coil measurement system [14]. Table 2 summarizes the geometrical harmonics at a field gradient of ~100 T/m with a reference radius of 17 mm. Harmonics for TQC02Ea are also shown for comparison. One can see that the magnetic field measurements in TQC02Eb do not show any specific distortions related to the dipole style collar design.

Estimates of the conductor residual resistivity ratio (RRR) were made during the magnet warm-up. The total coil RRR is 205±5, while the inner layer and the outer layer RRR values are 200 and 210 respectively.

The measured variations of coil RRR for the reference model TQC02Ea was 209-230.

IV. Conclusion

The first TQ magnet built with dipole style collars was successfully built and tested at Fermilab The dipole style structure achieved the same final preloads as the traditional quadrupole structure with significantly shorter assembly time and reduced risk of coil damage.

Quench performance and field quality of TQC02Eb are consistent with the test results for models built with quadrupole style collars (TQC02Ea) and those based on the shell (TQS02a/c) structure.

Harmonic measurements do not show any significant anomalies related to the dipole style collar design.

The TQC program at Fermilab has demonstrated that the yoke-supported collared coil assembly can be used with brittle Nb_3Sn coils. The dipole style collar structure can be easily adopted for long Nb_3Sn quadrupole (and dipole) magnets. This approach will be efficient during LHC performance upgrades, allowing the replacement of NbTi coils with Nb_3Sn coils in the same mechanical structure to increase aperture, reduce magnet length, increase magnet temperature margin or any combination of these features.

The next step is to assemble and test in FY2011 a 4-m long quadrupole based on dipole style collars using recycled LARP LQ coils [15].

Acknowledgment

The authors thank the technical staff of Fermilab's Technical Division for their contributions to magnet fabrication and test.

References

[1] R. Bossert et al., "Development of a High Gradient Quadrupole for the LHC Interaction Regions", *IEEE Transactions on Applied Superconductivity*, Vol. 7, No 2, pp. 751-754, June 1997.

[2] A.V. Zlobin et al., "Magnet Designs for Muon Collider Ring and Interaction Regions", Proc. of IPAC'10, Kyoto, Japan, May 2010, p.388.

[3] R.C. Bossert et al., "Development of TQC01, a 90mm Nb3Sn Model Quadrupole for LHC Upgrade Based on SS Collar," in *IEEE Transactions on Applied Superconductivity*, Vol 16, No 2, pp. 370-373, June 2006.

[4] S. Feher et al., "Development and Test of LARP Technological Quadrupole (TQC) Magnet", *IEEE Transactions on Applied Superconductivity*, vo. 17, No. 2, pp. 1126-1129, June 2007.

[5] R.C. Bossert et al., "Development and Test of LARP Technological Quadrupole Models of TQC Series", *IEEE Transactions on Applied Superconductivity*, Vol. 18, No 2, pp. 175-178, June 2008.

[6] R. Bossert et al., "Fabrication and Test of LARP Technological Quadrupole Models of TQC series," IEEE Transactions on Applied Superconductivity, Volume 19, Issue 3, June 2009 Page(s): 1226 - 1230.

[7] Gourlay, S.A., et al., "Magnet R&D for the US LHC Accelerator Research Program (LARP)," in *IEEE Transactions on Applied Superconductivity*, Vol. 16, No 2, pp 324-327, June 2006.

[8] S. Caspi, et al.., "Design and construction of TQS01, a 90mm Nb3Sn Quadrupole Model for LHC Luminosity Upgrade Based on a Key and Bladder Structure," in *IEEE Transactions on Applied Superconductivity*, Vol. 16, No 2, pp. 358-361, June 2006.

[9] N.I. Andreev et al., "Development and Study of the UNK Superconducting Quadrupole Magnet, *Proceedings of the European Particle Accelerator Conference*, pp. 2280-2282, 1994.

[10] A.I. Ageev et al., "The Development and Study of Superconducting Magnets for the UNK", *IEEE Transactions on Magnetics*, Vol. 28, No. 1, 1992, p. 182.

[11] G. Spigo et al, "Design and Performance of a new 50mm Quadrupole Magnet for the SSC", *Supercollider 5*, Plenum Press, N.Y., pp. 647-651, 1994.

[12] R. Bossert et al., "Development and Test of Collaring Methods for Nb3Sn Quadrupole Magnets", CEC/ICMC'2009, Tucson, AZ, June 2009.

[13] N. Andreev et al.,"Quench performance of Fermilab High Gradient Quadrupole short models for the LHC interaction regions", PAC'99, New York, April 1999, p. 3197.

[14] G. V. Velev et al., "A Fast Continuous Magnetic Field Measurement System based on Digital Signal Processors", IEEE Trans. Appl. Superconduct., Vol. 12, Issue 2, June 2006, pp 1374-1377

[15] G. Ambrosio et al., "Development and Coil Fabrication for the LARP 3.7-m Long Nb3Sn Quadrupole", *IEEE Transactions on Applied Superconductivity*, Volume 19, Issue 3, June 2009 Page(s): 1231 - 1234